The serine/threonine kinase PknB of *Mycobacterium tuberculosis* phosphorylates PBPA, a penicillin-binding protein required for cell division

Arunava Dasgupta,† Pratik Datta,† Manikuntala Kundu and Joyoti Basu

Department of Chemistry, Bose Institute, 93/1 Acharya Prafulla Chandra Road, Kolkata 70 0009, India

Correspondence
Joyoti Basu
joyoti@vsnl.com

A cluster of genes encoded by ORFs Rv0014c–Rv0018c in *Mycobacterium tuberculosis* encodes candidate cell division proteins RodA and PBPA, a pair of serine/threonine kinases (STPKs), PknA and PknB, and a phosphatase, PstP. The organization of genes encompassing this region is conserved in a large number of mycobacterial species. This study demonstrates that recombinant PBPA of *M. tuberculosis* binds benzylpenicillin. Knockout of its counterpart in *M. smegmatis* resulted in hindered growth and defective cell septation. The phenotype of the knockout (PBPA-KO) could be restored to that of the wild-type upon expression of PBPA of *M. tuberculosis*. PBPA localized to the division site along with newly synthesized peptidoglycan, between segregated nucleoids. *In vivo* coexpression of PBPA and PknB, *in vitro* kinase assays and site-specific mutagenesis substantiated the view that PknB phosphorylates PBPA on T362 and T437. A T437A mutant could not complement PBPA-KO. These studies demonstrate for the first time that PBPA, which belongs to a subclass of class B high-molecular-mass PBPs, plays an important role in cell division and cell shape maintenance. Signal transduction mediated by PknB and PstP likely regulates the positioning of this PBP at the septum, thereby regulating septal peptidoglycan biosynthesis.

INTRODUCTION

Tuberculosis causes more than two million deaths per year. Faced with this global threat it is crucial to better understand the physiology of the causative organism, *Mycobacterium tuberculosis*, in order to develop efficient therapeutic strategies. Phosphorylation remains the best-studied reversible modification of proteins that plays a major role in signal transduction and regulation of biological functions. Prokaryotes predominantly use the two-component signal transduction system, comprising a signal sensor histidine kinase domain and a response regulator (Stock *et al.*, 2000). Ser/Thr/Tyr-specific protein phosphorylation represents one of the fundamental regulatory mechanisms in eukaryotes (Krebs & Fischer, 1989). Genomics has now documented the presence of Ser/Thr protein kinases (STPKs) in prokaryotes as well (Leonard *et al.*, 1998; Madec *et al.*, 2002; Shi *et al.*, 1998). *M. tuberculosis* has 11 putative STPKs, one phospho-Ser/Thr phosphatase and two Tyr phosphatases (Cole *et al.*, 1998). Eight of the 11 STPKs identified in the *M. tuberculosis* genome appear to be transmembrane proteins, with a putative extracellular sensor domain and an intracellular kinase domain. Among these, PknA, PknB, PknD, PknE, PknF, PknG and PknH catalyse autophosphorylation (Av-Gay *et al.*, 1999; Chaba *et al.*, 2002; Cowley *et al.*, 2004; Koul *et al.*, 2001; Molle *et al.*, 2003; Ortiz-Lombardia *et al.*, 2003; Peirs *et al.*, 1997), and conserved phosphorylated residues within the activation loop are necessary for activity (Duran *et al.*, 2005). Two recent reports have identified Wag31, the mycobacterial orthologue of *Bacillus subtilis* DivIVA, as a substrate of PknA (Kang *et al.*, 2005), and GarA as a substrate of PknB (Villarino *et al.*, 2005). PknH has been shown to phosphorylate EmbR, which is a putative transcriptional activator that belongs to the OmpR-like family (Molle *et al.*, 2003), whereas PknF phosphorylates an ABC transporter encoded by Rv1747 (Molle *et al.*, 2004).

---

†These authors contributed equally to this work.

Abbreviations: DAPI, 4′,6-diamino-2-phenylindole; MBP, myelin basic protein; PBP, penicillin-binding protein; PBPA-KO, *M. smegmatis* inactivated in the *pbpA* gene; PknB-KD, PknB-Kin with a deletion of amino acid residues V95–D194 (i.e. kinase-dead); PknB-Kin, cytosolic kinase domain of PknB; STPK, serine/threonine protein kinase; WGA, wheat germ agglutinin.

A supplementary figure showing an alignment of the deduced amino acid sequences of the PBPA orthologues from different mycobacteria is available with the online version of this paper.

The final stages of peptidoglycan synthesis are carried out by penicillin-binding proteins (PBPs), a group of serine acyl transferases involved in cell wall expansion, cell shape maintenance, septum formation and cell division (Goffin & Ghuysen, 1998; Popham & Young, 2003). Höltje (1998) postulated the existence of distinct holoenzyme complexes for cell division and elongation. *M. tuberculosis* has the ability to shift from a state of active replication to a latent state with minimum replication. It is likely that the regulation of cell wall synthesis and cell division in response to varying environmental conditions is central to this process.

Based on *in silico* analyses and sequence/motif similarity-based clustering, the ORF Rv0016c encodes a putative PBP, PBPA, which belongs to a cluster termed class B-like I (Goffin & Ghuysen, 2002). PBPA lacks one conserved motif in the N-terminal module. Comparison of the derived amino acid sequences of PBPA from different mycobacterial species shows that this protein is highly conserved among *M. tuberculosis*, *Mycobacterium leprae*, *Mycobacterium bovis*, *Mycobacterium avium* subsp. *paratuberculosis* and *Mycobacterium smegmatis* (see supplementary Fig. S1, available with the online version of this paper). This suggests that the role of this protein is likely to be conserved among mycobacteria. We have focused our present studies on PBPA and its possible regulation by the STPK PknB (encoded by Rv0014c), and PstP (encoded by Rv0018c), a serine/threonine phosphatase (Av-Gay & Everett, 2000) similar to the PP2C family of enzymes. Our results support the idea that signal transduction by serine/threonine kinases and phosphatases provides a novel means of regulating cell septation and cell shape in mycobacteria, and possibly other Gram-positive bacteria that harbour counterparts of these proteins.

METHODS

Molecular biological procedures. Standard procedures were used for cloning and analysis of DNA, PCR and transformation. Electroporation in mycobacteria was carried out using a Bio-Rad Gene Pulser according to the protocol of Snapper *et al.* (1990). Cosmid MTCY10H4 was a generous gift from Stewart Cole, Institut Pasteur, Paris, France. Enzymes used to manipulate DNA were from Roche Applied Sciences. All constructs made by PCR were sequenced to verify their integrity.

Bacterial strains and growth conditions. *Escherichia coli* strains were grown in Luria–Bertani (LB) Miller (Difco) medium. Mycobacterial strains were grown in Middlebrook (MB) 7H9 (Difco) or Lemco medium (per litre: 5 g Lemco powder, 5 g NaCl, 10 g Bacto peptone) (Parish *et al.*, 2001) supplemented with 0·05 % Tween 80. Antibiotics were used at the following concentrations: ampicillin, 75 μg ml^{-1}; kanamycin monosulfate, 50 μg ml^{-1} for *E. coli* and 25 μg ml^{-1} for *M. smegmatis*; and hygromycin B, 100 μg ml^{-1} for *E. coli* and 50 μg ml^{-1} for *M. smegmatis*.

Genetic manipulations. *pbp*A (Rv0016c) was amplified from cosmid MTCY10H4 using the primer pair 5′-TTGGATCCCATATGAACGC-CTCTCTGCGCCGA-3′(sense) and 5′-TTGAATTCTCATGGTTCCC-CCTGCAG-3′(antisense), and cloned between the asymmetric *Bam*HI

and *Eco*RI sites (underlined) of pK19 to generate pJBA201. After sequencing, the gene was excised with *Bam*HI and *Eco*RI and cloned between the same sites of pET28a to generate pJBA202.

The gene encoding the cytosolic kinase domain of PknB (M1–V276) [PknB-Kin] was amplified from MTCY10H4 using the primer pair 5′-AAATACATATGACCACCCCTTCCCA-3′ (sense) and 5′-TT-CTCGAGCACGCGGACCAGGTCGGC-3′ (antisense), and cloned between the asymmetric *Nde*I and *Xho*I sites (underlined) of pET28a to generate pJBA302. To create a deletion within the catalytic kinase core of PknB, pJBA302 was digested with *Sal*I and a 297 bp fragment encoding V95–D194 was discarded. The larger fragment was gel-purified and religated to generate pJBA303.

To coexpress PBPA and PknB-Kin of *M. tuberculosis*, both the genes were cloned at the two multiple cloning sites (MCS) of pET Duet-1 (Novagen). Briefly, *pbpA* with the N-terminal His tag was excised from pJBA202 using *Nco*I and *Hin*dIII and cloned in the MCS1 of pET Duet-1 at the same sites to generate pJBA203. The *pknB-kin* gene was excised from pJBA302 using *Nco*I and *Xho*I and cloned in pBAD mycHisB (Invitrogen) between the same sites to generate pJBA204 encoding *pknB-kin* carrying a C-terminal myc epitope. This gene was then amplified by PCR using the primers 5′-TTGGATCCAATG ACCAC-CCCTTCCCA-3′(sense) and 5′-ATGGAATTCTCAGTCGACGGCG-CATTCAGATC-3′ (antisense). The amplicon was digested with *Bam*HI (underlined) and cloned in the MCS2 of pJBA203 between the *Bgl*II and *Eco*RV sites to generate pJBA205. A similar strategy was employed to generate the plasmid pJBA206 encoding *pbpA* and *myc-pknB-KD*. The sequences of all clones were confirmed by DNA sequencing.

Expression and purification of PknB-Kin and PknB-KD. Transformed cells were grown to an OD$_{600}$ of 0·6. IPTG was added to a final concentration of 0·1 mM, and growth was continued at 37 °C with shaking for 2 h. Cells were harvested and broken by sonication in 10 mM Tris/HCl, pH 7·5, containing 1 mM MgCl$_2$, 1 μg DNase ml^{-1}, 1 μg leupeptin, 1 ml^{-1} μg aprotinin ml^{-1}, 1 μg pepstatin ml^{-1} and 1 mM Pefabloc. The post-sonicate supernatant was loaded on a Ni^{2+}-NTA-agarose column equilibrated with 50 mM sodium phosphate, pH 7·4, containing 0·5 M NaCl (buffer A). After washing the column with 100 mM imidazole in buffer A, PknB-Kin was eluted with 200 mM imidazole in buffer A. PknB-KD was similarly expressed and purified.

Expression and purification of PBPA. *E. coli* BL21(DE3)/ pJBA202 was grown to an OD$_{600}$ of 0·6. IPTG was added to a final concentration of 0·1 mM, and growth was continued at 37 °C with shaking for 4 h. Cells after sonication were centrifuged at 5000 *g* for 5 min, the pellet was discarded and membranes were pelleted from the supernatant by centrifugation at 100 000 *g* for 1 h. PBPA was extracted by suspension of membranes in 10 mM Tris/HCl (pH 8) containing 1 % (w/v) cetyltrimethylammonium bromide (CTAB) at 4 °C for 40 min. After centrifugation at 100 000 *g* for 30 min, the supernatant was removed and loaded on to a 1 ml Ni^{2+}-NTA agarose column equilibrated with buffer A. After washing the column with buffer A containing 100 mM imidazole, PBPA was eluted with a gradient of 100–200 mM imidazole/1 % (w/v) CTAB in buffer A. All steps were carried out at 4 °C.

Penicillin-binding assays. Purified 6 × His-tagged PBPA (His-PBPA) or membranes from cells expressing PBPA were analysed by SDS-PAGE, Coomassie blue staining and fluorography of the gels after labelling of the protein with different concentrations of benzyl[^{14}C]penicillin for 30 min at 37 °C as described by Granier *et al.* (1994).

***In vitro* kinase assay.** Purified PknB-Kin (1 μg) was added to a 25 μl reaction volume containing 2 μg purified PBPA (or its

derivatives) in kinase buffer (25 mM Tris/HCl, pH 7·5, 5 mM β-glycerophosphate, 2 mM DTT, 2 mM MnCl$_2$, 0·1 mM sodium orthovanadate). The reaction was started by addition of 1 µCi (37 kBq) [γ-^{32}P]ATP (Jonaki, Board of Radiation and Isotope Technology, Hyderabad, India), continued at 25 °C for 30 min and stopped by adding 5 µl 5× Laemmli sample buffer. The samples were boiled and separated by SDS-PAGE. Gels were dried and exposed to Kodak XAR film for autoradiography. In some experiments, proteins separated by SDS-PAGE were electrotransferred and Western blotting was performed using monoclonal anti-phosphothreonine (Sigma), anti-phosphoserine (Sigma) or anti-phosphotyrosine (Cell Signalling Technology) antibody.

Coexpression of PBPA and PknB-Kin and analysis of phosphorylation. *E. coli* BL21(DE3) transformed with either pJBA205 or pJBA206 was grown at 37 °C to mid-exponential phase. Induction was started by the addition of IPTG (0·05 mM) and growth was continued for 4 h at 37 °C. Induced samples were denatured with SDS gel denaturing buffer, separated by SDS-PAGE, transferred to PVDF membranes and blotted with anti-His antibody to check the expression of His-PBPA. The membrane was then reprobed with anti-myc antibody to confirm the expression of myc-tagged PknB-Kin or PknB-KD. To analyse the phosphorylation of both PBPA and PknB, proteins were extracted from the induced cells harbouring either pJBA205 or pJBA206 using Cell Lytic BII bacterial extraction reagent (Sigma) according to the manufacturer's recommendations. Extracted proteins were separated by 10 % SDS-PAGE, transferred to PVDF membranes and blotted with anti-phosphothreonine monoclonal antibody in order to detect the phosphorylated threonine residues. Membranes were reprobed with anti-His or anti-myc antibody to confirm the identity of the bands as PBPA and PknB respectively.

Construction of truncated derivatives of PBPA, site-directed mutagenesis, expression and purification. A 690 bp fragment encoding amino acid residues M1–G229 of PBPA was excised from pJBA202 with *Bam*HI and *Not*I and cloned between the same sites in pET28a, generating pJBA207. A 1·1 kb fragment encoding amino acid residues L127–P491 of PBPA was excised from pJBA202 using *Nru*I and *Eco*RI, and cloned between the *Pvu*II and *Eco*RI sites of pBADHisB (Invitrogen), generating pJBA208. pJBA208 was digested with *Nco*I and *Eco*RI and the fragment encoding 6×His-tagged [L127–P491]PBPA was cloned between the same sites of pET28a to generate pJBA209. To generate truncated constructs, the gene fragments encoding E240–E320, Q316–P491, P346–Q420 and V383–P491 of PBPA were amplified using the sense (s) and antisense (as) primer pairs 5′-ATGGATCCATGGAACAGCTGACTGCGGCG-3′ (s) and 5′-ATGAATTCTTCCGCCACTTGCAGCGG-3′ (as); 5′-ATGGATCC-ATGCAAGTGGCGGAATCAACC-3′ (s) and 5′-ATGAATTCTCATG-GTTCCCCCTGCAG-3′(as); 5′-ATGGATCCATGCCGCTAGCGAAC-GCAGAA-3′ (s) and 5′-ATGAATTCCTGCACGCCGGGGATTGC-3′ (as); and 5′-ATGGATCCATGGTCGGATACCAGCAGCGC-3′ (s) and 5′-ATGAATTCTCATGGTTCCCCCTGCAG-3′ (as) respectively. All amplicons were cloned between the asymmetric *Bam*HI and *Eco*RI sites of pET28a. The genes encoding [Q316–P491]PBPA harbouring mutations T362A, or T437A, or T362A and T437A, in pET28a, were generated by the principle of overlap extension PCR, giving rise to pJBA216, pJBA217 and pJBA218 respectively. To generate constructs carrying the mutated full-length *pbpA* genes in pET vectors, pJBA216 or pJBA217 or pJBA218 was digested with *Nhe*I (located 1038 bp downstream from the start of the *pbpA* gene) and *Eco*RI, and the resulting fragment was first cloned between the *Nhe*I and *Eco*RI sites of pJBA201. The mutated full-length *pbpA* genes were then excised from these constructs and cloned between the *Bam*HI and *Eco*RI sites of pET28a. For dual expression in pET-DUET, the mutated genes along with the 6×His-encoding sequence were PCR-amplified from the pET28a-derived constructs and cloned between

the *Nco*I and *Eco*RI sites of pJBA205 (replacing the wild-type gene) to generate constructs harbouring the mutated PBPA genes and the gene for PknB-Kin.

The constructs of *pbpA* (truncations or point mutations) in pET-28a were expressed by induction with 0·1 mM IPTG for 3 h at 37 °C and purified by chromatography on Ni^{2+}-NTA agarose.

Construction of a suicidal delivery vector for inactivation of PBPA in *M. smegmatis*. A *pbpA* deletion mutant of *M. smegmatis* was constructed employing the allelic replacement method of Parish & Stoker (2000) using p2NIL, the gene-manipulating vector without any mycobacterial origin of replication, and pGOAL19, the marker gene cassette-containing vector. For disruption of *pbpA* of *M. smegmatis*, a suicidal delivery vector, pJBA104, was constructed. Briefly, 2083 bp of DNA fragment containing flanking sequences upstream from the start and downstream from the end of the *pbpA* gene was PCR amplified using the genomic DNA of wild-type *M. smegmatis* mc^{2}155 as template and the primer pair 5′-TACAACATTTTCGA-CCACGTG-3′ (sense) and 5′-TAT<u>GGATCC</u>GGACAGCGTGAC-3′ (antisense). The amplicon was cloned in pUC19 between the *Bam*HI (underlined) and *Sma*I sites to give pJBA101. To create an in-frame deletion construct lacking amino acid residues G47–E222 (including the active-site serine) pJBA101 was digested with *Sma*I and *Sca*I, a 525 bp fragment was eliminated and the 4240 bp larger fragment was religated to generate pJBA102. The truncated *pbpA* gene was excised from pJBA102 and cloned in p2NIL between the *Pml*I and *Bam*HI sites to generate pJBA103. The final delivery vector, pJBA104, was generated by excising the *Pac*I cassette (*hyg*, pAg85-*lacZ*, phsp60-*sacB*), which confers blue colour, hygromycin resistance and sucrose sensitivity, from the vector pGOAL19 and cloning it into pJBA103 bearing the truncated *pbpA* allele.

Isolation of the *pbpA*-inactivated mutant. pJBA104 was electroporated into electrocompetent cells of *M. smegmatis* mc^{2}155. The cells after electroporation were revived in 1 ml Lemco broth for 3 h and then plated on Lemco agar supplemented with hygromycin B, kanamycin and X-Gal (50 mg ml^{-1}). Blue colonies were streaked onto Lemco agar without any selection to enhance the recombination process. Cells were then plated onto Lemco agar supplemented with 2 % sucrose and 50 mg X-Gal ml^{-1}. The white colonies were restreaked onto replica plates containing X-Gal and sucrose, either without or with kanamycin and hygromycin. Genomic DNA was prepared from the white, Kan^S, Hyg^S, Suc^R colonies generated by double crossover. Genotype was analysed by PCR using genomic DNA from mc^{2}155 or from the Kan^S, Hyg^S and Suc^R colonies as template and the primer pair 5′-ATCATGGTGTTGATCGTGCTG-3′(sense) and 5′-TCCTGCAGCGACACGGTGGGT-3′ (antisense) which flanked the deletion site.

Complementation of PBPA of *M. tuberculosis* in the PBPA-KO strain using an integrating vector. Complementation of PBPA was achieved by constructing the integrating vector pJBA105, which contains a hygromycin-resistance cassette along with a positive-selection L5 integrase cassette. For this, first *pbpA* was cloned in pOLYG under control of the *hsp60* promoter to generate pJBA106. *hsp60*-*pbpA* was excised from pJBA106 by digesting with *Xba*I and *Hin*dIII and cloned in pUC19 between the sites for these two enzymes to give pJBA107. A 3·757 kb Hyg-integrase cassette was excised from pUC-HY-INT (Mahenthiralingam *et al.*, 1998) by digesting with *Hin*dIII and cloned at the single *Hin*dIII site of pJBA107 to generate the integrating vector pJBA105. pJBA105 was electroporated into electrocompetent cells of *pbpA*-inactivated *M. smegmatis* in order to complement the mutated *pbpA* with a single copy of the wild-type *pbpA*. The presence of *pbpA* was confirmed by PCR with *pbpA*-specific primers.

Complementation of PBPA by ectopic expression in the PBPA-KO strain. Complementation of the *pbpA* genes in the *pbpA*-inactivated *M. smegmatis* was carried out as follows. Briefly, the 6 × His-*pbpA* gene or its T362A, T437A mutant was cloned in pCKB115 (Choudhuri *et al.*, 2002) harbouring an *hsp60* promoter. The genes along with the *hsp60* promoter were excised with *Xba*I and *Hind*III and cloned between the same sites of pOLYG (Gaora *et al.*, 1997). For ectopic expression of PBPA or its mutant, the respective constructs were electroporated into *pbpA*-inactivated *M. smegmatis* (designated PBPA-KO). Expression of PBPA was confirmed by Western blotting of the membranes with anti-His antibody.

Growth curve analysis. Starter cultures were prepared by inoculating *M. smegmatis* mc^{2}155 or its derivatives from glycerol stocks into Lemco medium. These starter cultures were used to inoculate liquid media to a theoretical OD_{600} value of 0·05. Cultures were grown at 37 °C in a shaking incubator and samples were collected at different time intervals, passed five times under sterile conditions through a 26-gauge needle and vortexed. Serial dilutions were plated on Lemco agar plates to determine the number of c.f.u. after incubation at 37 °C.

Electron microscopy. Exponential-phase cultures of different *M. smegmatis* strains were harvested, washed three times with 0·15 M cacodylate buffer, treated with 1 % osmium tetroxide for 1 h at room temperature, centrifuged, and the collected cells were fixed with 0·15 M cacodylate buffer containing 2 % glutaraldehyde for 2 h at room temperature. Cells were again collected after centrifugation and fixed overnight with 0·15 M cacodylate buffer containing 1 % osmium tetroxide at 4 °C. The cells were dehydrated using graded ethanol (10 %, 30 %, 50 %, 70 % and 100 %), mounted on microscope stubs and sputter coated on the sputter coater. The samples were then examined under a Leica S440 scanning electron microscope.

Fluorescence microscopy. Immunostaining was adapted from the method of Harry *et al.* (1995) with a few modifications. Cells were fixed by incubation for 15 min at room temperature and 45 min on ice in 2·5 % (v/v) paraformaldehyde, 0·04 % (v/v) glutaraldehyde, 30 mM sodium phosphate (pH 7·5). After washing in PBS, the cells were permeabilized by exposing to 2 % toluene for 2 min, and immediately transferred to slides. The slides were washed with PBS, air-dried, dipped in methanol (-20 °C) for 5 min and then in acetone (-20 °C) for 30 s and allowed to dry. After rehydration with PBS, the slides were blocked for 2 h at room temperature with 2 % (w/v) BSA-PBS and incubated for 1 h with appropriate dilution of anti-His antibody in BSA-PBS. The slides were washed extensively with PBS and then incubated with a 1 : 1000 dilution of Alexa 488-conjugated anti-rabbit IgG (Molecular Probes) in BSA-PBS. For staining of DNA, 2 µg 4′,6-diamino-2-phenylindole (DAPI) ml^{-1} or 0·1 µg propidium iodide ml^{-1} was included with the secondary antibody. When propidium iodide was used to stain DNA, the slides were incubated in 100 µg RNase A ml^{-1} in PBS to remove RNA from the preparation. Wheat germ agglutinin (WGA)-Alexa Fluor 488 (Molecular Probes) (2 µg ml^{-1}) was used for staining of cell walls (Sizemore *et al.*, 1990). WGA is a lectin that binds to oligomers of *N*-acetylglucosamine and *N*-acetylmuramic acid. After extensive washing with PBS, the slides were mounted using 50 % glycerol. In controls for assessing specificity of the secondary antibodies, the incubation with the primary antibodies was omitted.

Protein phosphatase assay. The catalytic domain of PstP was cloned, expressed and purified as described by Boitel *et al.* (2003). Dephosphorylation of phosphorylated PBPA or myelin basic protein (MBP) was assayed as described by Boitel *et al.* (2003) with some modifications. Phosphorylated PBPA and MBP were obtained by performing the kinase reaction using [γ-^{32}P]ATP and PknB as described above. Dephosphorylation assays were carried out in a 25 µl reaction mixture containing 50 mM HEPES buffer pH 7·5, 0·1 mM EDTA, 1 mM DTT and 5 mM MnCl$_2$. The reaction was started with the addition of purified PstP (100 ng per 25 µl) and incubated for different periods of time at 30 °C. The reaction was terminated by adding SDS gel denaturing buffer and boiling for 10 min. Proteins were separated by SDS-PAGE and the disappearance of radiolabelled bands corresponding to phosphorylated PBPA or MBP was monitored by autoradiography. In separate experiments, dephosphorylation was carried out in the presence of 50 mM NaF.

RESULTS

Expression of PBPA in *E. coli*, its extraction, purification and [^{14}C]penicillin binding of His-PBPA

To validate the function of the putative PBPA protein as a PBP, the gene Rv0016c was cloned in the vector pET28a, expressed as 6 × His-tagged PBPA, and purified as described. The purified PBPA was > 95 % homogeneous as determined by SDS-PAGE (Fig. 1a). Purified His-PBPA bound benzyl-[^{14}C]penicillin in a concentration-dependent manner, reaching saturation at a penicillin concentration of 10^{-4} M (Fig. 1b), validating its function as a PBP. Membrane-associated PBPA bound benzyl[^{14}C]penicillin with a similar affinity (Fig. 1b). The membrane-associated PBP and the purified protein therefore appeared to be functionally indistinguishable.

Identification of the counterpart of PBPA of *M. tuberculosis* in the *M. smegmatis* genome and construction of a *pbpA* mutant of *M. smegmatis*

PBPA was found to be conserved across pathogenic and non-pathogenic mycobacterial species (see supplementary Fig. S1), suggesting that its function too was likely to be conserved. In view of this, we chose the fast-growing non-pathogenic *M. smegmatis* as a model organism to investigate
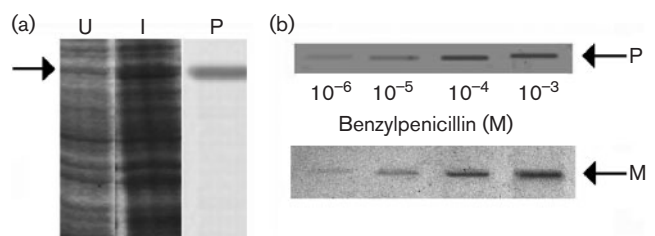

Fig. 1. Expression, purification and penicillin binding of PBPA of *M. tuberculosis*. (a) Coomassie blue-stained gel of uninduced (U) and induced (I) cells of *E. coli* expressing PBPA, and purified His-PBPA (P). The arrow indicates the position of expressed PBPA in the induced cells. (b) Fluorogram of the binding of purified (P) or membrane-bound (M) His-PBPA to different concentrations of benzyl[^{14}C]penicillin. Purified PBPA or membrane from cells expressing PBPA was treated with different concentrations of benzyl[^{14}C]penicillin and separated by SDS-PAGE, followed by fluorography.
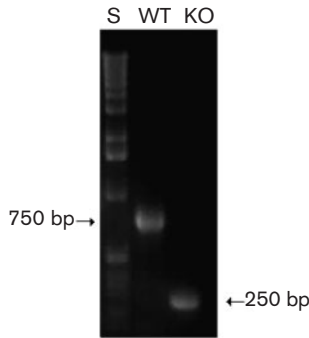
S WT KO

750 bp→

←250 bp

Fig. 2. PCR analysis of the wild-type and *pbpA* knockout strain of *M. smegmatis*. Chromosomal DNA isolated from the wild-type *M. smegmatis* mc²155 (WT) or its knockout mutant *pbp*A-KO (KO) was used as template for PCR analysis using primers described in Methods. The sizes of PCR products were analysed by agarose gel electrophoresis followed by ethidium bromide staining. Lane S contains 1 kb ladder.

the role of PBPA in mycobacterial physiology. PBPA of *M. smegmatis* showed 74 % identity in amino acid sequence with PBPA of *M. tuberculosis*. The inactivation of *pbpA* of *M. smegmatis* was therefore undertaken in order to study its consequence in this model organism.

The suicidal delivery vector pJBA104 (harbouring a truncated *M. smegmatis pbpA* gene) was used for homologous recombination. As expected in the event of successful inactivation of *pbpA*, a 250 bp PCR product was obtained in the case of two of the transformants, as opposed to a 750 bp PCR product in the case of wild-type mc²155 (Fig. 2). The PCR products were sequenced to verify the identity of the bands and the deletion within the *pbpA* gene. The mutated strain will be referred to as PBPA-KO.

Effect of inactivation of PBPA of *M. smegmatis*

To investigate the effect of inactivation of the *pbpA* gene, the morphology and the growth rates of wild-type mc²155 and

PBPA-KO were compared. Unlike wild-type cells, PBPA-KO was unable to grow in synthetic medium. It was routinely grown in Lemco medium. PBPA-KO exhibited reduced growth compared to the wild-type in Lemco broth supplemented with 0·05 % Tween 80. The wild-type reached mid-exponential phase at 20 h, whereas the *pbpA* mutant reached mid-exponential phase at 24 h. Moreover, the growth of the mutant was approximately twofold lower than that of the wild-type at stationary phase (Fig. 3a). These findings suggested that PBPA is required for maintenance of total cell mass. The *in vitro* growth of the mutant strain on Lemco solid medium and on slants was poor compared to that of the wild-type strain.

Mid-exponential-phase cells of the wild-type and the mutant both grown in Lemco medium were viewed by scanning electron microscopy. Most of the cells (>90 %) of the PBPA-KO strain were 3·5 to 4 times longer than those of the wild-type (Fig. 4).

Complementation of *pbpA* of *M. tuberculosis* in the PBPA-KO strain and its effect on growth and morphology

To assess the ability of PBPA of *M. tuberculosis* to complement the growth defect of PBPA-KO, a single copy of His-*pbpA* of *M. tuberculosis* was integrated into the chromosome of *M. smegmatis* using the integrating vector pJBA105 harbouring the His-*pbpA* gene under the control of the *hsp60* promoter. The presence of the integrated gene was confirmed by PCR, and the complemented strain was observed to display growth characteristics and colony morphology similar to that of the wild-type. Expression of His-PBPA was analysed by Western blotting using anti-His antibody. The expression was very weak, prompting us to favour ectopic expression of His-PBPA of *M. tuberculosis* as a tool for immunolocalization analysis. Expression of plasmid-encoded His-PBPA was confirmed by Western blotting of membranes from the complemented strain with anti-His antibody (Fig. 3b). The signal was stronger than that of the integrated His-PBPA. All experiments were
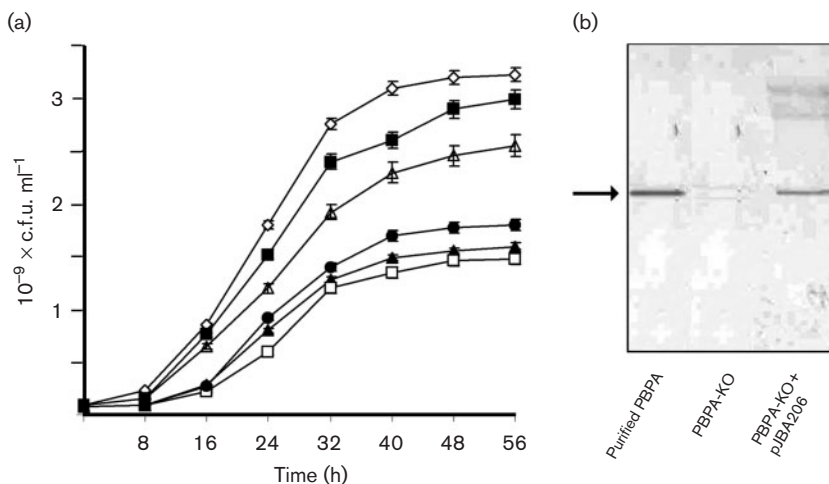

(a)

$10^{-9} \times$ c.f.u. ml^{-1}

Time (h)

(b)

Purified PBPA

PBPA-KO

PBPA-KO+ pJBA206

Fig. 3. (a) Growth kinetics of *M. smegmatis* mc²155 and its derivatives: wild-type mc²155 (◇), PBPA-KO (□) and PBPA-KO complemented with pOLYG harbouring the genes of wild-type *pbpA* of *M. tuberculosis* (■) or the mutants T362A (△), T437A (●), or T362A, T437A (▲). The results are means±SE of three experiments (some of the error bars are smaller than the symbols). (b) Expression of PBPA in the complemented strain. Membranes from PBPA-KO and PBPA-KO complemented with wild-type His-tagged *pbpA* (PBPA-KO + pJBA206), and purified PBPA, were separated by SDS-PAGE followed by Western blotting using anti-His-antibody. The arrow indicates the position of His-PBPA.
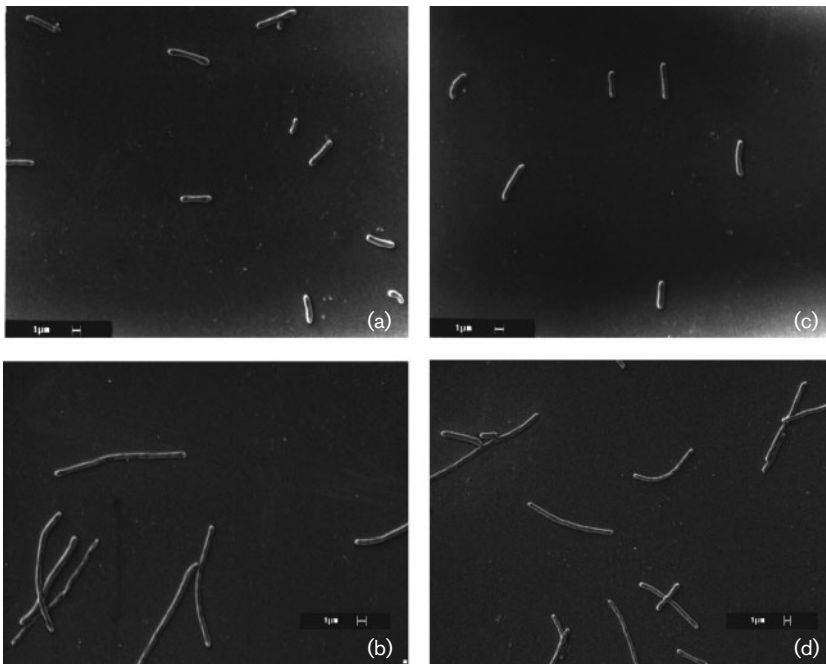
Fig. 4. Scanning electron micrographs of (a) *M. smegmatis* mc²155 (wild-type), (b) *pbpA* knockout mutant (PBPA-KO), (c) PBPA-KO complemented with wild-type *pbpA* and (d) PBPA-KO complemented with *pbpA*(T437A). Bars, 1 μm.

subsequently performed with the plasmid-encoded system. PBPA-KO complemented with plasmid-encoded His-PBPA showed a substantial recovery of growth characteristics, approaching that of the wild-type (Fig. 3a). Scanning electron microscopy showed that the complemented cells regained wild-type morphology (Fig. 4), confirming the role of PBPA in maintenance of normal cell growth and morphology, and supporting the view that PBPA of *M. tuberculosis* and *M. smegmatis* fulfil similar functions.

Staining of PBPA-KO cells with WGA-Alexa Fluor 488

WGA-Alexa Fluor 488 staining is useful for visualizing cell wall and septa. Fluorescence-labelled WGA binds specifically to *N*-acetylglucosamine in the outer peptidoglycan layer of Gram-positive bacteria (Sizemore *et al.*, 1990), including *M. smegmatis*. WGA-Alexa Fluor 488 staining of the PBPA-KO strain failed to detect staining between nucleoids (Fig. 5a–c), indicating that peptidoglycan synthesis had not occurred at the expected position of septa. This view was supported by the observation that the mutant contained a larger average number (4 ± 1) of nucleoids per cell. The majority of the cells of the knockout strain (80 %) showed 4 nucleoids per cell.

Immunolocalization of PBPA

To visualize PBPA in PBPA-KO complemented with *pbpA* of *M. tuberculosis*, the cells were incubated with anti-His antibody followed by incubation with Alexa-546-conjugated secondary antibody. Cells from exponential-phase cultures of the wild-type mc²155 and PBPA-KO were subjected to the same treatments to serve as negative controls. In most of the cells, bright red fluorescent patches attributable to the

presence of His-PBPA were observed at mid-cell (Fig. 5d). To demonstrate that the anti-His antibody was reacting specifically with His-PBPA, cells from exponential-phase cultures of the wild-type and PBPA-KO were subjected to the same treatments. No red fluorescence was observed in either of these cells (data not shown). Nucleoids were visualized by staining with DAPI (blue) (Fig. 5f). Staining with WGA-Alexa 488 (Fig. 5e) showed formation of septal peptidoglycan between nucleoids. Overlaying the three images obtained by staining for PBPA (red), for peptidoglycan (green) and for nucleoids (blue) showed that PBPA colocalizes (yellow) with newly formed septal peptidoglycan in the gap between segregated nucleoids (Fig. 5g) in the case of the complemented strain. These observations clearly suggested that PBPA localizes to the septum. To exclude the possibility that the His tag directs PBPA to mid cell, an irrelevant His-tagged protein was expressed in *M. smegmatis* PBPA-KO. This protein could not be located at mid-cell (data not shown).

Coexpression of PknB and PBPA of *M. tuberculosis* in *E. coli* and evidence that PBPA is phosphorylatable by PknB

The interest in PBPA and PknB arises from the fact that they are encoded by neighbouring ORFs, one being a protein likely to be important in cell division and growth, the other an STPK. PknB is a 626 aa transmembrane protein with an intracellular N-terminal kinase domain and an extracellular C-terminal domain. The kinase domain of PknB has been crystallized (Young *et al.*, 2003). Boitel *et al.* (2003) have demonstrated that the kinase domain of PknB undergoes autophosphorylation, shows a preference for Mn^{2+} as the divalent cation required for kinase activity, and
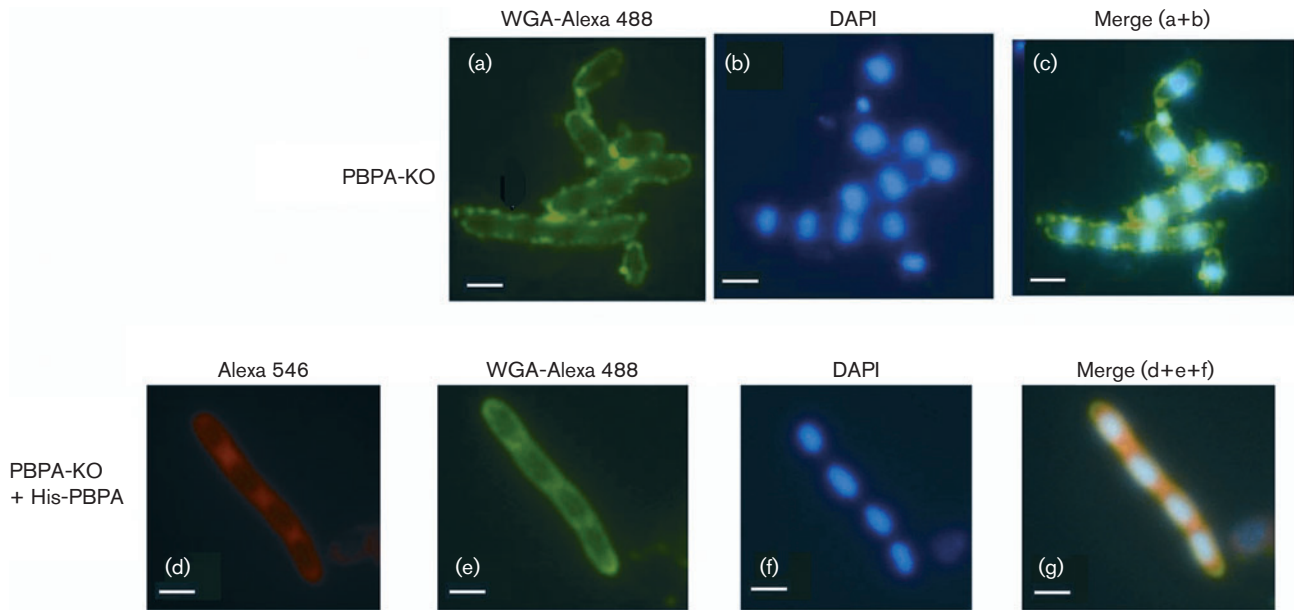
Fig. 5. Fluorescence microscopy of *pbpA*-inactivated *M. smegmatis* (PBPA-KO). *M. smegmatis* (PBPA-KO) (a–c) or PBPA-KO complemented with wild-type His-PBPA of *M. tuberculosis* (d–g) were stained with WGA-Alexa 488 (green) (a, e) for staining cell wall and septa, or with DAPI (b, f) for visualizing nucleoids. Immunological localization of His-PBPA in the complemented strain was carried out by incubating with anti-His antibody followed by staining with Alexa 546-conjugated mouse IgG (red; d). In PBPA-KO complemented with *pbpA*, WGA-Alexa 488 staining detected completed septa (e) and Alexa 546 showed the localization of PBPA (d). Merging of (d), (e) and (f) (panel g) showed the colocalization of PBPA with completed septa (yellow) between nucleoids. Formation of completed septa was absent in PBPA-KO cells (a, c). Bars, 2 µm.

phosphorylates the model substrate MBP. We attempted to address the question whether PBPA is an endogenous substrate of PknB. The coexpression of His-PBPA and myc-PknB-Kin (or myc-PknB-KD) in *E. coli* was visualized by Western blotting using anti-His (Fig. 6a) and anti-myc (Fig. 6b) antibodies. Using this dual expression system, we tested whether PBPA is phosphorylatable by PknB. Electrophoretically separated extracts of coexpressed proteins developed positive bands after probing with anti-phosphothreonine antibody when the kinase domain of PknB was coexpressed with PBPA, but not when its kinase-dead counterpart was coexpressed (Fig. 6c). The lack of phosphorylation of PBPA when it was coexpressed with a kinase-inactive mutant of PknB confirmed the specificity of the phosphorylation of PBPA by PknB. No bands developed when anti-phosphoserine antibody was used to detect phosphorylation of PBPA by PknB (data not shown), indicating that phosphorylation occurred specifically on threonine residues.

Purification and characterization of PknB in *E. coli* and phosphorylation of PBPA by the kinase domain of PknB

As reported by Boitel *et al.* (2003), recombinant, purified PknB-Kin (Fig. 6d) was capable of autophosphorylation and also phosphorylated MBP *in vitro* in the presence of Mn^{2+} (Fig. 6e). On the other hand, PknB-KD did not

undergo autophosphorylation and could not phosphorylate MBP under similar conditions. We next tested whether PBPA was a direct substrate for PknB, by performing an *in vitro* kinase assay using purified proteins. Phosphorylation of PBPA was observed in the presence of PknB-Kin, but not in the presence of PknB-KD (Fig. 6e).

Determination of the site(s) of PknB-mediated phosphorylation of PBPA

Considering that PknB appeared to phosphorylate PBPA on threonine residues, we attempted to map the site(s) of PknB-mediated phosphorylation of PBPA. Primary sequence analysis revealed the presence of 38 threonine residues in PBPA. The NetPhos 2.0 program available at http://www.cbs.dtu.dk (Blom *et al.*, 1999) was used to map putative phosphorylatable threonine residues. Five putative high-scoring threonine residues at positions 26, 223, 314, 362, 437 were identified as candidate phosphorylatable residues. A number of His-tagged truncated constructs as well as threonine point mutants of PBPA were generated covering the entire PBPA amino acid sequence. The results of *in vitro* kinase assays using these constructs are summarized in Table 1. The candidate phosphorylatable residues predicted by NetPhos in each construct are indicated. Taking together the results obtained with each construct, T437 and T362 appeared to be the two residues that were phosphorylated by PknB. The results of *in vitro* phosphorylation of the
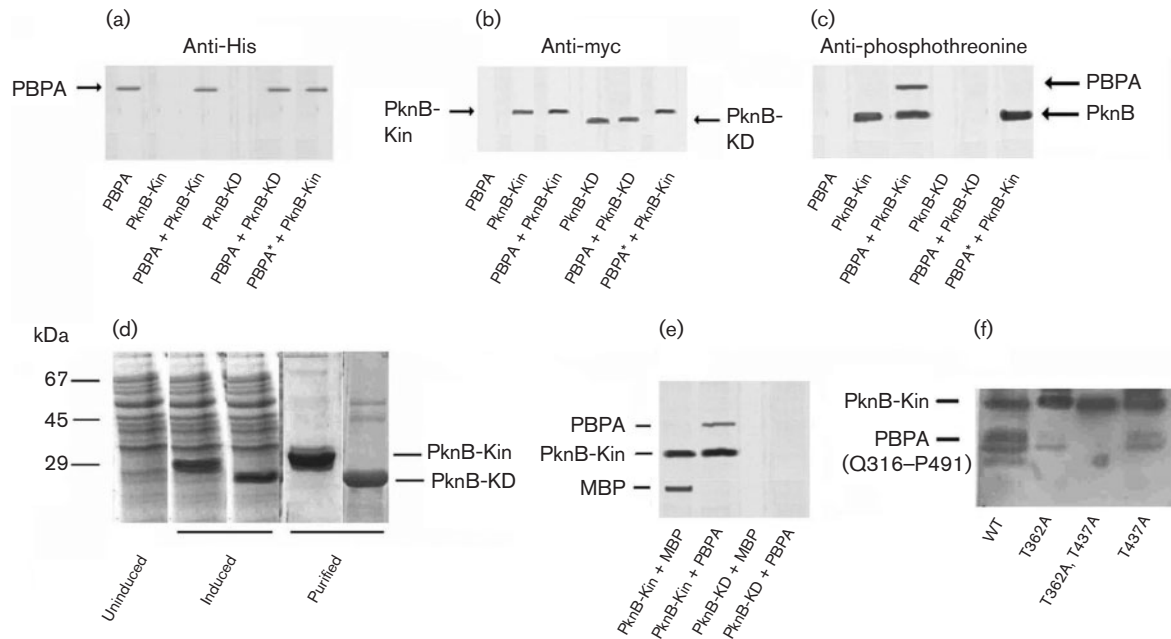
Fig. 6. Phosphorylation of PBPA by PknB. Cell lysates from cells expressing His-PBPA or myc-PknB-Kin or myc-PknB-KD alone; or coexpressing His-PBPA [or the double mutant His-PBPA(T362A, T437A), denoted as PBPA*] and myc-PknB constructs were separated by SDS-PAGE, electrotransferred and subjected to Western analysis using anti-His (a), anti-myc (b) and anti-phosphothreonine (c) antibody. Arrows indicate the positions of the respective bands. (d) Coomassie blue-stained gels of uninduced cells of *E. coli*, induced cells expressing PknB-Kin (second lane) or Pkn B-KD (third lane); purified PknB-Kin (fourth lane) or PknB-KD (fifth lane). (e) *In vitro* phosphorylation of MBP or PBPA by PknB-Kin or PknB-KD. (f) *In vitro* phosphorylation of mutants of PBPA by PknB-Kin. WT represents the PBPA construct spanning amino acid residues Q316–P491. Site-directed mutants are derivatives of this construct. For (e) and (f), purified PknB-Kin (or PknB-KD) was used to phosphorylate PBPA constructs in the presence of $[\gamma\text{-}^{32}\text{P}]$ATP (e) or non-radioactive ATP (f). Reactions were stopped by denaturing in SDS gel denaturing buffer; proteins were separated and subjected to autoradiography (e) or electrotransferred and probed with antiphosphothreonine antibody (f).

truncated construct [Q316–P491]PBPA (or its threonine mutants) by PknB-Kin followed by Western blotting with anti-phosphothreonine antibody are depicted in Fig. 6(f). No band was observed in the T362A, T437A double mutant. Bands were obtained using the construct [Q316–P491]PBPA when only one of the two threonine residues at positions T437 or T362 was mutated to alanine, indicating that PknB-mediated phosphorylation occurred at both these residues. Coexpression of PBPA(T362A, T437A) with PknB-Kin in *E. coli* showed that this mutant was not phosphorylated by PknB (Fig. 6c). Taken together, these results clearly indicated that threonines 362 and 437 of PBPA of *M. tuberculosis* represent the residues phosphorylatable by PknB.

Consequences of mutation of the PknB-phosphorylatable threonine residues of PBPA

To investigate the role of phosphorylation of PBPA of *M. tuberculosis*, The PBPA-KO strain was complemented with *M. tuberculosis pbpA* encoding proteins carrying the T437A or T362A, or T362A,T437A (double) mutation. The genes encoding these constructs were harboured in pOLYG under the control of the *hsp60* promoter. Growth kinetics of the

pbpA(T437A)-complemented mutant as well as the *pbpA*-(T362A,T437A)-complemented strain resembled that of PBPA-KO. The growth of the *pbpA*(T362A)-complemented mutant was intermediate between that of the wild-type and the *pbpA* mutant (Fig. 3a). CLUSTAL W analysis of the sequences of PBPA of different mycobacterial species showed that T437 was conserved across slow- and fast-growing species. On the other hand, T362, while being conserved in *M. tuberculosis*, *M. bovis*, *M. leprae* and *M. avium* subsp. *paratuberculosis*, was not conserved in *M. smegmatis* (supplementary Fig. S1). It therefore appeared likely that phosphorylation at T437 could play an essential role in regulating cell division across mycobacterial species. Taking this together with the fact that the T437A mutant failed to complement PBPA-KO, we focused our attention on the effects of complementation of PBPA-KO with PBPA (T437A) on cell morphology and localization of PBPA. When PBPA-KO was complemented with His-*pbpA*(T437A), the cells remained unaltered in morphology as observed by scanning electron microscopy (Fig. 4). His-PBPA(T437A) failed to localize to the septum when observed by immunofluorescence microscopy of the complemented strain. WGA-Alexa 488 and DAPI staining revealed a lack of

Table 1. Results of *in vitro* phosphorylation of different constructs of PBPA with PknB

Amino acid residues encompassed in PBPA construct	Candidate phosphorylatable threonine residue(s)*	Phosphorylation by PknB
M1–G229	T26, T223	−
R127–P491	T223, T314, T345, T362, T437	+
E240–P491	T314, T345, T362, T437	+
Q316–P491	T345, T362, T437	+
E240–E320	T314	−
G323–Q420	T345, T362	+
P346–Q420	T362	+
V383–P491	T437	+
E240–E320 (T314A)	None	−
G323–Q420 (T345A)	T362	+
P346–Q420 (T362A)	None	−
V383–P491 (T437A)	None	−
Q316–P491 (T437A)	T345, T362	+
Q316–P491(T362A)	T345, T437	+
Q316–P491 (T345A, T437A)	T362	+
Q316–P491 (T362A, T437A)	T345	−

*Candidate phosphorylatable threonine residues were identified using NetPhos 2.0.

†−, No detectable phosphorylation; +, phosphorylation detected after *in vitro* kinase assays with PknB-Kin followed by probing with anti-phosphothreonine antibody.

septum formation and an increase in the average number of nucleoids per cell, just as observed in the case of PBPA-KO (data not shown).

Dephosphorylation of phosphorylated PBPA by PstP

PstP belongs to the PP2C family of serine/threonine phosphatases, which are characterized by their dependence on the divalent cations Mg^{2+} or Mn^{2+} (McCarty & Chory, 2000; Pullen *et al.*, 2004). Given that reversible protein phosphorylation provides a ubiquitous signalling mechanism that defines the response to changing environmental conditions, we asked the question whether PknB and PstP could exert opposing effects on PBPA to coordinately regulate cell division. To address this question, purified PBPA was phosphorylated by PknB using radiolabelled ATP. The phosphorylated protein was then incubated with purified PstP. Phosphorylated MBP was also used as a positive control. The time-dependent disappearance of the label associated with both MBP and PBPA (Fig. 7) confirmed that MBP and PBPA could both be dephosphorylated by PstP. NaF, a known phosphatase inhibitor, inhibited the PstP-mediated

dephosphorylation of both these proteins (Fig. 7). This confirmed the specificity of the PstP-mediated dephosphorylation reaction.

DISCUSSION

Prokaryotic genes involved in the same cellular processes are often clustered, forming an operon. The presence of the genes encoding the kinases PknA and PknB, the phosphatase PstP, the class B-like PBP PBPA, the putative cell division gene *rodA* and two forkhead-associated (FHA) domain-containing proteins (Durocher & Jackson, 2002; Durocher *et al.*, 2000) in a gene cluster in *M. tuberculosis* strengthened the view that these are likely to be involved in coordinated regulation of cell division and/or cell elongation. The genomic region encompassing these genes is conserved in *M. leprae* (in spite of extensive gene decay in this species), *M. avium* subsp. *paratuberculosis* and *M. bovis*, as well as in fast-growing mycobacteria such as *M. smegmatis* (Fsihi *et al.*, 1996; Salazar *et al.*, 1996). The conservation of these genes argues in favour of an essential role of the encoded proteins in cell function, possibly related to cell growth. Sassetti *et al.* (2003) suggested that PknB and PknA are likely to be required for the growth of *M. tuberculosis in vitro*.

Cell growth and development require the cell wall to have a dynamic structure. PBPs are crucial for the synthesis of peptidoglycan in specific phases of growth or development, underscoring the need to elucidate the functions of the
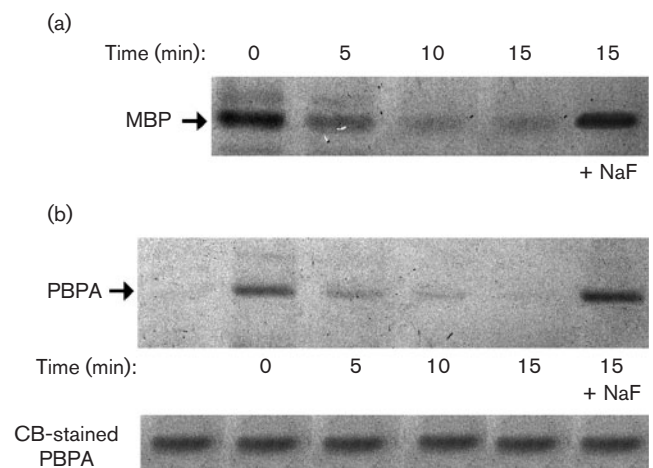

Fig. 7. Dephosphorylation of phosphorylated MBP and PBPA by PstP. PBPA or MBP was phosphorylated using $[\gamma\text{-}^{32}\text{P}]$ATP and PknB as described in Fig. 6. Phosphorylated MBP (a) or PBPA (b) was incubated in the presence of PstP at 30 °C and aliquots were withdrawn at intervals as indicated, followed by boiling in the presence of SDS gel denaturing buffer. Proteins were separated by SDS-PAGE, followed by autoradiography. The last lanes in both (a) and (b) represent reactions carried out in the presence of the phosphatase inhibitor NaF. The lower gel of (b) represents Coomassie blue-stained PBPA indicating equal loading in all lanes.

mycobacterial PBPs. *pbpA*, *pknB* and *pstP* are cotranscribed (Kang *et al.*, 2005), raising the possibility that PBPA could be regulated by reversible phosphorylation. Expression of PBPA in *E. coli*, its purification and analysis of penicillin binding confirmed that PBPA is a bona fide PBP. A mutant of *M. smegmatis* inactivated in the counterpart of the *pbpA* gene required nutrient-rich medium for growth and grew more slowly than the wild-type, suggesting that PBPA likely plays an important role during the active phase of growth. This was supported by the observation of Betts *et al.* (2002) that *pbpA* is downregulated during nutrient starvation. His-PBPA expressed ectopically in the mutant localized to the septum along with newly synthesized peptidoglycan, implying that it plays a role in cell division. Studies with *E. coli* and *Haemophilus influenzae* lend support to the view that cell wall synthesis is executed by two distinct holoenzyme complexes, one involved in elongation and the other in division (Alaedini & Day, 1999; Höltje, 1998). *E. coli* PBP3 is the classical transpeptidase demonstrated to be essential for peptidoglycan synthesis at the division site (Weiss *et al.*, 1999). However, several PBPs from different bacterial species such as *B. subtilis* (Scheffers *et al.*, 2004) and *E. coli* (PBP2) (Den Blaauwen *et al.*, 2003) have been shown to localize to the lateral cell wall as well as to the septum in dividing cells. Although our immunofluorescence studies failed to localize PBPA to the lateral wall, we do not rule out the possibility that the fluorescence signals may have been too weak to be visible at the periphery.

PknB-mediated phosphorylation of PBPA suggested that this modification may modulate the function of PBPA in regulating cell division. T362 and T437 were identified as the residues phosphorylatable by PknB. The preferred substrate motif predicted by Kang *et al.* (2005) using a proteomic approach was not corroborated by our studies. In agreement with the observations of Kang *et al.* (2005), PknB phosphorylated PBPA on threonine but not on serine residues. However, the two sites of phosphorylation identified by us did not carry a Q at the +1 position, the preferred amino acid residue predicted by Kang *et al.* (2005) from peptide library screening data. Although PBPA carries a single TQ motif within the sequence NATMT^{26}QVFT, T26 was not phosphorylated by PknB (Table 1). On the other hand, T437 was predicted as a putative phosphorylation site by NetPhos (Blom *et al.*, 1999). Our studies suggest that the elegant peptide library screening methods used by Kang *et al.* (2005) do not exclude the possibility of identification of additional substrates of PknB.

T362 was conserved among the slow-growing species of mycobacteria, namely *M. leprae*, *M. bovis*, *M. tuberculosis*, and *M. avium* subsp. *paratuberculosis*, but replaced by an alanine in *M. smegmatis*. On the other hand, T437 was conserved across all species of mycobacteria for which the genomes have been sequenced. The single T437A mutation in PBPA made the protein incapable of complementing the growth and morphological defects of the PBPA-KO strain. The failure of the T437A mutant to localize to the site of

division suggested that PknB-mediated phosphorylation targets PBPA to the septum. This appeared likely considering that *M. smegmatis* PknB was 65 % identical to *M. tuberculosis* PknB and the kinase domains of the two PBPs shared 86 % identity. We argued that PknB of *M. smegmatis* could probably exert the same effect on ectopically expressed PBPA of *M. tuberculosis* as PknB of *M. tuberculosis* would do to endogenous PBPA. This was supported by our unpublished observations that recombinant PknB (kinase domain) of *M. smegmatis* phosphorylated recombinant PBPA of *M. tuberculosis in vitro*.

Boitel *et al.* (2003) and Chopra *et al.* (2003) have shown that the catalytic domain of PknB is inactivated by dephosphorylation by PstP, the phosphatase present in the same operon. Our present report documents that PBPA is also a substrate of PstP. It appears possible that dephosphorylation of PBPA by PstP may shuttle it to another location within the cell, leading to the termination of cell division. Identification of PBPA as a substrate of PknB and PstP, together with the fact that inactivation of PBPA leads to impaired growth kinetics and altered morphology of the cells, suggests that this cluster of genes regulates growth and division of mycobacteria and related members of the GC-rich Gram-positive bacteria.

The role of signalling molecules in cell division or in cell growth has remained largely elusive. Reversible phosphorylation-dependent coordinated regulation of cell division and cell fate has been established in *B. subtilis*. Reversible phosphorylation of anti-sigma factor SpoIIAA (Duncan & Losick, 1993; Duncan *et al.*, 1995, 1996) regulates its binding to σ^F, thereby regulating transcription. SpoIIE is also required for normal formation of the asymmetrically positioned septum during *B. subtilis* sporulation (Lucet *et al.*, 2000). The CckA, PleC and DivJ histidine kinases are dynamically localized to the cell poles of *Caulobacter crescentus*, each at distinct stages of the cell cycle (Jacobs *et al.*, 1999; Wheeler & Shapiro, 1999). In a recent study, the pole-to-pole oscillation of the signalling molecule DivK has been elegantly demonstrated to be controlled by the kinase DivJ and the phosphatase PleC in *C. crescentus* (Matroule *et al.*, 2004). Collectively these reports indicate that signal transduction pathways via histidine kinases, serine/threonine kinases and phosphatases influence growth, cell division and segregation in many organisms. Understanding the precise mechanism involved in the localization of phosphorylated PBPA to the septum, as well as the defined physiological signal leading to PknB-mediated PBPA phosphorylation, needs further investigation.

ACKNOWLEDGEMENTS

REFERENCES

Alaedini, A. & Day, R. A. (1999). Identification of two penicillin-binding multienzyme complexes in *Haemophilus influenzae*. *Biochem Biophys Res Commun* **264**, 191–195.

Av-Gay, Y. & Everett, M. (2000). The eukaryotic-like Ser/Thr protein kinases of *Mycobacterium tuberculosis*. *Trends Microbiol* **8**, 238–244.

Av-Gay, Y., Jamil, S. & Drews, S. J. (1999). Expression and characterization of the *Mycobacterium tuberculosis* serine/threonine protein kinase PknB. *Infect Immun* **67**, 5676–5682.

Betts, J. C., Lukey, P. T., Robb, L. C., McAdam, R. A. & Duncan, K. (2002). Evaluation of a nutrient starvation model of *Mycobacterium tuberculosis* persistence by gene and protein expression profiling. *Mol Microbiol* **43**, 717–731.

Blom, N., Gammeltoft, S. & Brunak, S. (1999). Sequence and structure-based prediction of eukaryotic protein phosphorylation sites. *J Mol Biol* **294**, 1351–1362.

Boitel, B., Ortiz-Lombardia, M., Duran, R., Pompeo, F., Cole, S. T., Cervenansky, C. & Alzari, P. M. (2003). PknB kinase activity is regulated by phosphorylation in two Thr residues and dephosphorylation by PstP, the cognate phospho-Ser/Thr phosphatase, in *Mycobacterium tuberculosis*. *Mol Microbiol* **49**, 1493–1508.

Chaba, R., Raje, M. & Chakraborty, P. K. (2002). Evidence that a eukaryotic-type serine/threonine protein kinase from *Mycobacterium tuberculosis* regulates morphological changes associated with cell division. *Eur J Biochem* **269**, 1078–1085.

Chopra, P., Singh, B., Singh, R. & 8 other authors (2003). Phosphoprotein phosphatase of *Mycobacterium tuberculosis* dephosphorylates serine-threonine kinases PknA and PknB. *Biochem Biophys Res Commun* **311**, 112–120.

Choudhuri, B. S., Bhakta, S., Barik, R., Basu, J., Kundu, M. & Chakrabarti, P. (2002). Overexpression and functional characterization of an ABC (ATP-binding cassette) transporter encoded by the genes *drrA* and *drrB* of *Mycobacterium tuberculosis*. *Biochem J* **367**, 279–285.

Cole, S. T., Brosch, R., Parkhill, J. & 39 other authors (1998). Deciphering the biology of *Mycobacterium tuberculosis* from the complete genome sequence. *Nature* **393**, 537–544.

Cowley, S., Ko, M., Pick, N. & 8 other authors (2004). The *Mycobacterium tuberculosis* protein serine/threonine kinase PknG is linked to cellular glutamate/glutamine levels and is important for growth in vivo. *Mol Microbiol* **52**, 1691–1702.

Den Blaauwen, T., Aarsman, M. E., Vischer, N. O. & Nanninga, N. (2003). Penicillin-binding protein PBP2 of *Escherichia coli* localizes preferentially in the lateral wall and at mid-cell in comparison with the old cell pole. *Mol Microbiol* **47**, 539–547.

Duncan, L. & Losick, R. (1993). SpoIIAB is an anti-σ factor that binds to and inhibits transcription by regulatory protein σ^F from *Bacillus subtilis*. *Proc Natl Acad Sci U S A* **90**, 2325–2329.

Duncan, L., Alper, S., Arigoni, F., Losick, R. & Stragier, P. (1995). Activation of cell-specific transcription by a serine phosphatase at the site of asymmetric division. *Science* **270**, 641–644.

Duncan, L., Alper, S. & Losick, R. (1996). SpoIIAA governs the release of cell-type specific transcription by a serine phosphatase at the site of asymmetric division. *J Mol Biol* **260**, 147–164.

Duran, R., Villarino, A., Bellinzoni, M., Wehenkel, A., Fernandez, P., Boitel, B., Cole, S. T., Alzari, P. M. & Cervenansky, C. (2005). Conserved autophosphorylation pattern in activation loops and juxtamembrane regions of *Mycobacterium tuberculosis* Ser/Thr protein kinases. *Biochem Biophys Res Commun* **333**, 858–867.

Durocher, D. & Jackson, S. P. (2002). The FHA domain. *FEBS Lett* **513**, 58–66.

Durocher, D., Taylor, I. A., Sarbassova, D., Haire, L. F. & Jackson, S. P. (2000). The molecular basis of FHA domain : phosphopeptide binding specificity and implications for phospho-dependent signaling mechanisms. *Mol Cell* **6**, 1169–1182.

Fsihi, H., de Rossi, E., Salazar, L. & 7 other authors (1996). Gene arrangement and organization in an approximately 76 kb fragment encompassing the *oriC* region of the chromosome of *Mycobacterium leprae*. *Microbiology* **142**, 3147–3161.

Gaora, P., Bernini, S., Hayward, C., Filley, E., Rook, G., Young, D. & Thole, J. (1997). Mycobacteria as immunogens: development of expression vectors for use in multiple mycobacterial species. *Med Princ Pract* **6**, 91–96.

Goffin, C. & Ghuysen, J. M. (1998). Multimodular penicillin-binding proteins: an enigmatic family of orthologs and paralogs. *Microbiol Mol Biol Rev* **62**, 1079–1093.

Goffin, C. & Ghuysen, J. M. (2002). Biochemistry and comparative genomics of SxxK superfamily acyltransferases offer a clue to the mycobacterial paradox: presence of penicillin-susceptible target proteins versus lack of efficiency of penicillin as therapeutic agent. *Microbiol Mol Biol Rev* **66**, 702–738.

Granier, B., Jamin, M., Adam, M. & 15 other authors (1994). Serine-type D-Ala-D-Ala peptidases and penicillin-binding proteins. *Methods Enzymol* **244**, 249–266.

Harry, E., Pogliano, K. & Losick, R. (1995). Use of immunofluorescence to visualize cell-specific gene expression during sporulation in *Bacillus subtilis*. *J Bacteriol* **177**, 3386–3393.

Höltje, J. V. (1998). Growth of the stress-bearing and shape-maintaining murein sacculus of *Escherichia coli*. *Microbiol Mol Biol Rev* **62**, 181–203.

Jacobs, C., Domian, I. J., Maddock, J. R. & Shapiro, L. (1999). Cell cycle-dependent polar localization of an essential bacterial histidine kinase that controls DNA replication and cell division. *Cell* **97**, 111–120.

Kang, C.-M., Abbott, D. W., Park, S. T., Dascher, C. C., Cantley, C. & Husson, R. N. (2005). The *Mycobacterium tuberculosis* serine/threonine kinases PknA and PknB: substrate identification and regulation of cell shape. *Genes Dev* **19**, 1692–1704.

Koul, A., Choidas, A., Tyagi, A. K., Drlica, K., Singh, Y. & Ullrich, A. (2001). Serine/threonine protein kinases PknF and PknG of *Mycobacterium tuberculosis*: characterization and localization. *Microbiology* **147**, 2307–2314.

Krebs, E. G. & Fischer, E. H. (1989). The phosphorylase *b* to *a* converting enzyme of rabbit skeletal muscle. *Biochim Biophys Acta* **1000**, 302–309.

Leonard, C. J., Aravind, L. & Koonin, E. V. (1998). Novel families of putative protein kinases in bacteria and archaea: evolution of the "eukaryotic" protein kinase superfamily. *Genome Res* **8**, 1038–1047.

Lucet, I., Feucht, A., Yudkin, M. D. & Errington, J. (2000). Direct interaction between the cell division protein FtsZ and the cell differentiation protein SpoIIE. *EMBO J* **19**, 1467–1475.

Madec, E., Laszkiewic, Z. A., Iwanicki, A., Obuchowski, M. & Seror, S. (2002). Characterization of a membrane-linked Ser/Thr protein kinase in *Bacillus subtilis*, implicated in developmental processes. *Mol Microbiol* **46**, 571–586.

Mahenthiralingam, E., Marklund, B. I., Brooks, L. A., Smith, D. A., Bancroft, G. J. & Stokes, R. W. (1998). Site-directed mutagenesis of the 19-kilodalton lipoprotein antigen reveals no essential role for the protein in the growth and virulence of *Mycobacterium intracellulare*. *Infect Immun* **66**, 3626–3634.

Matroule, J. Y., Lam, H., Burnette, D. T. & Jacobs-Wagner, C. (2004). Cytokinesis monitoring during development: rapid pole-to-pole shuttling of a signaling protein by localized kinase and phosphatase in *Caulobacter*. *Cell* **118**, 579–590.

McCarty, D. R. & Chory, J. (2000). Conservation and innovation in plant signaling pathways. *Cell* **103**, 201–209.

Molle, V., Girard-Blanc, C., Kremer, L., Doublet, P., Cozzone, A. J. & Prost, J. F. (2003). Protein PknE, a novel transmembrane eukaryotic-like serine/threonine kinase from *Mycobacterium tuberculosis*. *Biochem Biophys Res Commun* **308**, 820–825.

Molle, V., Kremer, J., Girard-Blanc, C., Besra, G. S., Cozzone, A. J. & Prost, J. F. (2003). An FHA phosphoprotein recognition domain mediates protein EmbR phosphorylation by PknH, a Ser/Thr protein kinase from *Mycobacterium tuberculosis*. *Biochemistry* **42**, 15300–15309.

Molle, V., Soulat, D., Jault, J.-M., Grangeasse, C., Cozzone, A. J. & Prost, J.-F. (2004). Two FHA domains on an ABC transporter, Rv1747, mediate its phosphorylation by PknF, a Ser/Thr protein kinase from *Mycobacterium tuberculosi*s. *FEMS Microbiol Lett* **234**, 215–223.

Ortiz-Lombardia, M., Pompeo, F., Boitel, B. & Alzari, P. M. (2003). Crystal structure of the catalytic domain of the PknB serine/threonine kinase from *Mycobacterium tuberculosis*. *J Biol Chem* **278**, 13094–13100.

Parish, T. & Stoker, N. G. (2000). Use of a flexible cassette method to generate a double unmarked *Mycobacterium tuberculosis tlyA plcABC* mutant by gene replacement. *Microbiology* **146**, 1969–1975.

Parish, T., Turner, J. & Stoker, N. G. (2001). *amiA* is a negative regulator of acetamidase expression in *Mycobacterium smegmatis*. *BMC Microbiol* **1**, 19.

Peirs, P., De Wit, L., Braibant, M., Huygen, K. & Content, J. (1997). A serine/threonine protein kinase from *Mycobacterium tuberculosis*. *Eur J Biochem* **244**, 604–612.

Popham, D. L. & Young, K. D. (2003). Role of penicillin-binding proteins in bacterial cell morphogenesis. *Curr Opin Microbiol* **6**, 594–599.

Pullen, K. E., Ng, Ho-L., Sung, P.-Y., Good, M. C., Smith, S. M. & Alber, T. (2004). An alternate conformation and a third metal in PstP/Ppp, the *M. tuberculosis* PP2C-family Ser/Thr phosphatase. *Structure* **12**, 1947–1954.

Salazar, L., Fsihi, H., de Rossi, E., Riccardi, G., Rios, C., Cole, S. T. & Takiff, H. E. (1996). Organization of the origins of replication of the chromosomes of *Mycobacterium smegmatis*, *Mycobacterium leprae* and *Mycobacterium tuberculosis* and isolation of a functional origin from *M. smegmatis*. *Mol Microbiol* **20**, 283–293.

Sassetti, C., Boyd, D. H. & Rubin, E. J. (2003). Genes required for mycobacterial growth defined by high density mutagenesis. *Mol Microbiol* **48**, 77–84.

Scheffers, D.-J., Jones, L. F. & Errington, J. (2004). Several distinct localization patterns for penicillin-binding proteins in *Bacillus subtilis*. *Mol Microbiol* **51**, 749–764.

Shi, L., Potts, M. & Kennelly, P. J. (1998). The serine, threonine, and/or tyrosine-specific protein kinases and protein phosphatases of prokaryotic organisms: a family portrait. *FEMS Microbiol Rev* **22**, 229–253.

Sizemore, R. K., Caldwell, J. J. & Kendrick, A. S. (1990). Alternate Gram staining technique using a fluorescent lectin. *Appl Environ Microbiol* **56**, 2245–2247.

Snapper, S. B., Melton, R. E., Mustafa, S., Kieser, T. & Jacobs, W. R., Jr (1990). Isolation and characterization of efficient plasmid transformation mutants of *Mycobacterium smegmatis*. *Mol Microbiol* **4**, 1911–1919.

Stock, A. M., Robinson, V. L. & Gondreau, P. N. (2000). Two-component signal transduction. *Annu Rev Biochem* **69**, 183–215.

Villarino, A., Duran, R. Wehenkel A. & 8 other authors (2005). Proteomic identification of *M. tuberculosis* protein kinase substrates: PknB recruits GarA, a FHA domain-containing protein, through activation loop-mediated interactions. *J Mol Biol* **350**, 953–963.

Weiss, D. S., Chen, J. C., Ghigo, J. M., Boyd, D. & Beckwith, J. (1999). Localization of FtsI (PBP3) to the septal ring requires its membrane anchor, the Z Ring, FtsA, FtsQ, and FtsL. *J Bacteriol* **181**, 508–520.

Wheeler, R. T. & Shapiro, L. (1999). Differential localization of two histidine kinases controlling bacterial cell differentiation. *Mol Cell* **4**, 683–694.

Young, T. A., Delagoutte, B., Endrizzi, J. A., Falick, A. M. & Alber, T. (2003). Structure of *Mycobacterium tuberculosis* PknB supports a universal activation mechanism for Ser/Thr protein kinases. *Nat Struct Biol* **10**, 168–174.